Waveform Prediction of a Pulse Communication Link between Antennas Modeled by a Combination of Thin-wires

F. Sagnard[1] **and G. El-Zein**[2]
[1]IETR, INSA, France
[2]University of Marne-La-Vallée, France

Abstract—In the context of the development of the emerging Ultra-Wide Band (UWB) technology, the modelling and the analysis of the transient waveforms radiated and received in a communication link are proposed. The modelling developped, based on analytical expressions, allows to consider combinations of thin-wire elements to represent conductive antennas with a 2 D or 3 D geometry. The propagation channel has been modelled by the presence of a dielectric material in air. Detailed parametric studies have been performed, and optimization of the antenna characteristics has been addressed. This work appears as a synthesis and an extension of previous studies.

1. Introduction

In recent years, the Ultra-Wide Band (UWB) technology appears as an attractive solution for technical improvements in conventional narrow band wireless communication systems. Such a technology relies initially on the transmission of a series of baseband modulated (in amplitude or phase) short pulses (less than 1 ns) with a low duty cycle. Such signals have an energy which is spread thinly across the entire broadband spectrum (greater than 500 MHz with a fractional bandwidth of more than 20%), thus allowing the UWB technology to coexist with other wireless systems without licence. This technology offers several advantages such as: transmission at a high bit rate, low cost, low probabilities of interception and detection, separation of multipath... Therefore, several applications are being implemented including communications, networking, radar (GPR, vehicular, surveillance) imaging (medical, through-wall, construction materials, security, GPR), and measurement devices (sensors, positioning). Currently, the FCC has regulated UWB power levels emitted by defining a spectral mask in the -10 dB bandwidth between 3.1 and 10.6 GHZ in order to limit interferences with existent licensed wireless systems (WLANs, GPS). Efforts are under way by the IEEE community for standardizing the use of UWB systems in indoor (home and office) multimedia transmissions.

Because of the very wide frequency band of the transmitted signal, novel studies concerning the modelling and the characterization of the propagation channel and of the antennas have to be achieved; it appears that in such a case the studies are best performed in the time domain Therefore, we have focused our studies on the modelling and on the parameter analysis of the physical phenomena involved in the transient radiation, propagation and reception of a pulse signal in a simplified multipath propagation channel including a dielectric sample in air. The modelling tool uses extended analytical expressions, in the transmission and reception configurations, to describe the responses of conductive antennas made of a combination of infinitely and loaded linear thin-wire elements, representing several 2 D or 3 D antenna geometries (V-dipole, bow-tie, butterfly, TEM horn...). Such an original tool which includes extended developments of previous work allows to highlight the pulse-shaping process in the spatio-temporal domain [1, 3, 5].

2. Transient Responses of Thin-wire Elements

The basic transmission link is composed of single transmitting and receiving antennas separated by a distance d in the far-field zone of each other over the operating frequency bandwidth; the major component of the radiating field $E_\theta(r, \theta, \phi)$ is oriented along the direction $\vec{\theta}$. The antennas do not necessary face each other and can be tilted. The transmitting antenna is positioned at the origin 0, and two angles β and ϕ define the position of each wire element to axis Oz and axis Ox respectively. The propagation channel is modelled by the presence of a dielectric material with large dimensions which has been placed in the air between both antennas; thus, diffraction does not occur at the edges. The link modelled is presented in Figure 1 with the parameters associated with the frequency domain to highlight the presence of the several frequency-dependent impedances involved in the input and output circuits.

The modelling approaches described in this section concern in transmission symmetric straight dipoles $(-L, L)$, and in reception symmetric V-dipoles $(-L, L)$. In transmission, as the expressions allow to distinguish the radiated components of the electric field issued from each monopole, the extension of the modelling to a V-dipole can be easily deduced by tilting each arm. In reception, it appears more natural to model the physical phenomena involved in each arm individually. From the analytical expressions developed, other dipole orientations can be considered [2].

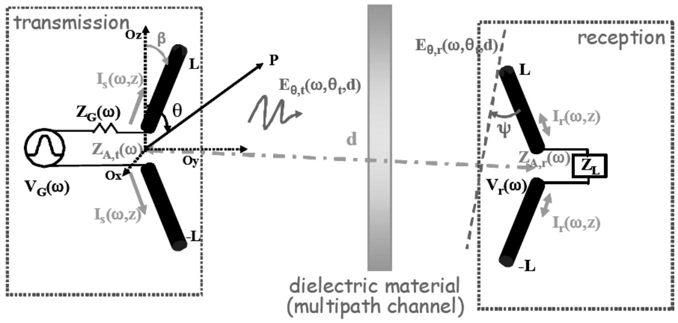

Figure 1: Geometry of the link between two V-dipoles with their parameters in the frequency domain.

2.1. Transmission Configuration

The straight dipole $(-L,\, L)$ aligned with axis Oz is supposed to be excited at the feed point $z = 0$ by an impulse current which has generally the shape of the Gaussian function or one of its successive derivatives. The p-th derivative $g(t)$ of the Gaussian function is expressed by:

$$g^{(p)}(t) = \frac{d^p}{dt^p}\left(A_0 e^{-(\frac{t}{\tau})^2}\right) \tag{1}$$

where τ represents the characteristic time of the pulse, and A_0 its amplitude. The duration w of each signal has been defined as the time interval centered on the pulse shape and containing 99% of the total energy of the pulse. For example, $w = 3.3\tau$ for $p = 0$, $w = 4.08\tau$ for $p = 1$, and $w = 4.5\tau$ for $p = 2$. In general, τ has been set in order to fit a number n not necessarily an integer of pulse durations in each arm length of the dipole. Thus, we defined the reference time $\tau_a = L/c = nw$, where c represents the velocity in the air.

In the case of an infinitely conductive dipole, the initial current wave $I_s(t - |z/c|)$ which propagates along both arms undergoes a total reflection (with a coefficient -1) as it reaches both terminations $z = L$ and $z = -L$, and a partial reflection at the feed point (denoted ρ). The back and forth propagation process continues until the traveling current undergoes a complete attenuation [1, 3]. Such a ringing effect produces narrow frequency radiated waveforms, and usually the objective is to reduce it as much as possible. In general, the dipole radiation is produced at the positions $z = 0$, $z = L$, and $z = L$. In the far-field zone, the main electric field component $E_\theta(r,\, \theta,\, t)$ in the spherical coordinates $(r,\, \theta)$ is expressed as follows [3]:

$$E_\theta(r,\theta,t) = \frac{\eta_0}{4\pi r}\left[\begin{array}{l}\sum\limits_{i=1}^{\infty}\Gamma_i\frac{\sin\theta}{(1-\cos\theta)}\{I_s(t-r/c-b_i) - I_s(t-r/c-(L/c)(1-\cos\theta)-b_i)\}\\ +\Gamma_i\frac{\sin\theta}{(1+\cos\theta)}\{I_s(t-r/c-c_i) - I_s(t-r/c-(L/c)(1-\cos\theta)-c_i)\}\end{array}\right] \tag{2}$$

$$b_i = \begin{cases}(L/c)(i-1+\cos\theta) & i \text{ even}\\ (L/c)(i-1) & i \text{ odd}\end{cases} \qquad c_i = \begin{cases}(L/c)(i-1-\cos\theta) & i \text{ even}\\ (L/c)(i-1) & i \text{ odd}\end{cases} \tag{3}$$

$$\Gamma_i = \begin{cases}(-1)^{i/2}\rho^{(i/2-1)} & i \text{ even}\\ (-\rho)^{(i-1)/2} & i \text{ even}\end{cases} \tag{4}$$

where η_0 represents the wave impedance in the vacuum. In relation (2), we can distinguish the contribution of both arms $(0, L)$ and $(0, -L)$ of the dipole to the radiated field induced by upward and downward propagating current components respectively: as the factor $\sin\theta/(1-\cos\theta)$ corresponds to the upper arm, the factor $\sin\theta/(1+\cos\theta)$ is associated with the lower arm. We notice that the total electric field radiated is built from differentiated delayed current components that express the time derivative of the current in each arm if the two components are separated by a delay $\Delta t = \tau_a(1-\cos\theta) \geq \omega$ and $\Delta t = \tau_a(1+\cos\theta) \geq \omega$. Also, we remark that the radiation of the lower arm is the same as the radiation of the upper arm when changing the observation angle θ to its complementary value $\pi - \theta$. Such a modeling has been compared to a numerical one based on the FIT, and the results agree satisfactorily.

In the case of a Wu and King (WK) loaded dipole, a distributed complex impedance along each arm length of the dipole is expressed by [4]:

$$Z(z,\omega) = \frac{1}{Y(z,\omega)} = r(0,\omega)\left(\frac{L}{L-|z|}\right)\left(1 - j\frac{k_0}{L}\right) \tag{5}$$

where k_0 is the wave number in the vacuum, and $r(0,\omega) = \frac{\eta_0\psi}{2\pi}$ the impedance at the feed-point $z = 0$ of the dipole. ψ is a function of the frequency, and η_0 the impedance of the free space. For the sake of simplicity, the parameter ψ is replaced by its mean value over the given frequency bandwith considered. The expression of the transient radiated electric field given by Samaddar et al. extended to consider the presence of an impedance associated with the input circuit is given by [5, 6]:

$$E_\theta(r,\theta,t) = \frac{1}{r\psi\sin^2\theta}\frac{\tau_a}{\tau_t}\begin{bmatrix} \sin^2\theta(V_G(t^*) - \frac{1}{\tau_t}\int_0^\infty V_G(t^*-t')e^{-t^0/\tau_t}dt' \\ -\frac{(1+\cos^2\theta)}{\tau_t}\int_0^\infty V_G(t^*-t')e^{-t^0/\tau_t}dt' \\ +\frac{(1+\cos\theta)^2}{2\tau_t}\int_0^\infty V_G(t_1-t')e^{-t^0/\tau_t}dt' \\ +\frac{(1-\cos\theta)^2}{2\tau_t}\int_0^\infty V_G(t_2-t')e^{-t^0/\tau_t}dt' \end{bmatrix} \tag{6}$$

where: $t^* = t - r/c$; $t_1 = t^* - \tau_a(1 - cos\theta)$; $t_1 = t^* - \tau_a(1 + cos\theta)$. Also, $\tau_t = C_g\tau_a$ with $C_g = 1 + 2\pi Z_G/(\eta_0\psi)$. Z_G is a constant representing the mean value of the impedance associated with the input circuit in the frequency bandwidth of the excitation signal. If $Z_G = 0$, we have $\tau_t = \tau_a$.

2.2. Reception Configuration

A dipole antenna $(-L, L)$ such as presented in Figure 1 is supposed to be excited at the upper arm by a transient electric plane wavefront with an oblique incidence angle ψ relative to the direction of the antenna. Two cases can be distinguished depending if a straight or a V-dipole is considered: in the case of a straight dipole, as the upper arm is first excited at its top, the lower arm is first excited at the position z = 0. In the case of a V-dipole, both upper and lower arms are first excited at their top. The analytical developments presented in this paper concern a monopole$(0, L)$ initially aligned with axis O_z. If the monopole is tilted with an angle β relative to axis O_z the expressions remain valid, and the case of a monopole $(0, -L)$ tilted with an angle $-\beta$ relative to axis O_z can be deduced from the expression of the upper monopole by adding an additional delay $\tau'_D = L\sin\psi/c$ and changing the incidence angle ψ by its complementary value $\pi - \psi$. The excitation signal $E_\theta(\theta_r, t)$, which is supposed to be issued from a transmitting antenna of the same kind, interacts with a given monopole $(0, L)$ and produces at each point of the element of abscissa z' an induced current $dI'(z, t; z')$. This current propagates from each excitation point z' in two opposite directions [2]. A time delay τ_D is assigned to each discrete source to represent the arrival time of the oblique plane wave front with incidence ψ on the antenna:

$$\tau_D = (L - z')\sin\psi/c \tag{7}$$

$$dI(z,t;z') = \left\{\begin{array}{c} dI'(z', t-(z-z')/c - \tau_D)\cos\psi \cdot U(z-z') \\ +dI'(z', t-(z+z')/c - \tau_D)\cos\psi \cdot U(z'-z) \end{array}\right\}[U(z) - U(z-L)] \tag{8}$$

where U is the Heaviside unit-step function. Each local current component mentioned in relation (8) writes as follows:

$$dI'(z',t) = Y(z')E(z', t-\tau_D) = 1/Z(z')E(z', t-(L-z')\sin\psi/c) \tag{9}$$

where $Z(z')$ represents the impedance which can vary along the antenna.

In the case of a uniform infinitely conductive antenna, we have extended previous developpement in order to consider the total current component distributed along the antenna arms for an oblique incidence. For the sake of simplicity the formulation concerning the upper monopole $(0, L)$ does not include the ringing e!ect issued from total and partial reflections at the top end and the feed point respectively:

$$\begin{aligned} I_{upper}(z,t) \quad = \quad & \frac{c\cos\psi}{1+\sin\psi}\{\xi(t-(L-z)\sin\psi/c) - \xi(t-z/c-L\sin\psi/c)\} \\ & + \frac{c\cos\psi}{-1+\sin\psi}\{\xi(t-(z-L)/c) - \xi(t+(z-L)\sin\psi/c)\} \end{aligned} \tag{10}$$

And $\xi(t) = \int_0^t E(t')dt'$. At the position $z = 0$, the current detected becomes:

$$I_{upper}(0,t) = -\frac{c\cos\psi}{1+\sin\psi}\xi(t-L\sin\psi/c) - \frac{c\cos\psi}{1-\sin\psi}\xi(t-L/c) + \frac{2c}{\cos\psi}\xi(t-L\sin\psi/c) \tag{11}$$

In the case of a WK loaded dipole, we have expressed the current generated by each local source along the upper monopole $(0, L)$ as follows:

$$dI'(z,t;z') = Y(z',t) \otimes E(z', t-(L-z')\sin\psi/c)\cos\psi \tag{12}$$

where $\otimes$ denotes the time convolution product. Then, replacing the local current $dI'(z, t; z')$ in relation (8),

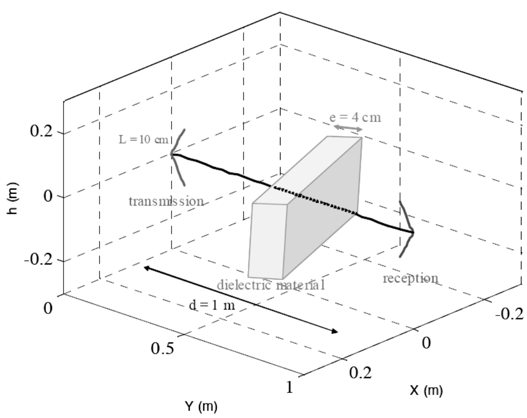

(a) Geometry of the link.

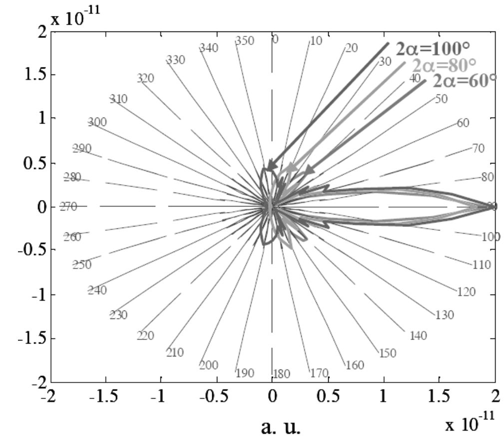

(b) Polar diagram of the radiated energy normalized for a V-dipole ($2L = 20\,\mathrm{cm}$).

Figure 2: (a) Geometry of the link simulated involving two V-dipoles in the far-field and a single-layer dielectric material; (b) Polar diagram of the radiated power of a uniform V-dipole for several aperture angles.

we obtain an additionnal component $I'_{upper}(z,\, t)$ which superimposes on the current component $I_{upper}(z,\, t)$ associated with the uniform monopole. It is defined as follows:

$$I'_{upper}(z,t) = I'_{top}(z,t) + I'_{bottom}(z,t) \tag{13}$$

$$\text{with:} \quad I'_{top}(z,t) = \frac{c\cos\psi}{1+\sin\psi}\left\{ \begin{array}{c} z\xi(t+(z-L)\sin\psi/c) \\ +\frac{1}{L}\frac{c}{1+\sin\psi}[\varsigma(t+(z-L)\sin\psi/c) - \varsigma(t-z/c-L\sin\psi/c)] \end{array} \right\} \tag{14}$$

$$I'_{bottom}(z,t) = -\frac{1}{L}\frac{c\cos\psi}{-1+\sin\psi}\left\{ \begin{array}{c} L\xi(t+(z-L)/c) - z\xi(t+z(z-L)\sin\psi/c) \\ +\frac{1}{L}\frac{c}{-1+\sin\psi}[\varsigma(t+(z-L)/c) - \varsigma(t+z/c-L\sin\psi/c)] \end{array} \right\} \tag{15}$$

And $\varsigma(t) = \int_0^t \xi(t')dt'$. Then the total current component without reflection at the feed-point is given by:

$$I_{WK,upper}(z,t) = \frac{1}{r(0)}(I_{upper}(z,t) + I'_{upper}(z,t)) \otimes e^{-t/\tau_a} \tag{16}$$

At the position $z = 0$, the current received by the detector is:

$$I_{WK,upper}(0,t) = \frac{1}{r(0)}(I_{upper}(0,t) + I'_{upper}(0,t)) \otimes e^{-t/\tau_a} \tag{17}$$

Relation (16) appears as a extended version of the expression given by Samaddar et al., [5], as it allows to study the current distribution along each arm of a dipole and not only at the position $z = 0$.

3. Simulation Results

As an illustration of the modelling presented above, we have considered in transmission and reception two identical symmetric V-dipoles formed of two thin-wire elements with length $L = 10\,\mathrm{cm}$ and characterized by an aperture angle $2\alpha = 120°$ ($\beta = 30°$) as presented in Figure 2(a). The dipoles which face each other have been fixed in each other far-field at a distance $d = 1\,\mathrm{m}$. The equivalent impedances at the feed-point in transmission and reception have been estimated to $600\,\Omega$. The excitation voltage in transmission is assumed to have the shape of the first derivative of the Gaussian function; the reference characteristic time τ has been fixed to 41.25 ps (which corresponds to the duration $\omega = 0.17\,\mathrm{ns}$), so that 2 pulses ($n = 2$) fit in each arm length L. The propagation channel is represented here by a single-layer dispersive dielectric material with thickness $e = 4\,\mathrm{cm}$; in the modelling, any multi-layer dielectric sample with a plane surface can be considered. In transmission, we have studied the influence of the aperture angle 2α, and the pulse duration (by the means of n) on the focalization of the electromagnetic energy radiated in the direction $\theta = 90°$. Some results associated with a uniform V-dipole are presented in Figure 2(b) for three angles $2\alpha = 60°$, $80°$, $100°$; they show that a focalization in the direction $\theta = 90°$ is obtained for $n = 2.9$, 1.7 and 0.9 pulses in a arm length $L = 10\,\mathrm{cm}$ (for $2\alpha = 120°$, we have found that $n = 0.8$). The polar diagram highlights that a narrower focalization is obtained for the lowest aperture angle 2α. Moreover, the spatio-temporal waveforms radiated in the far-field zone by a uniform (with

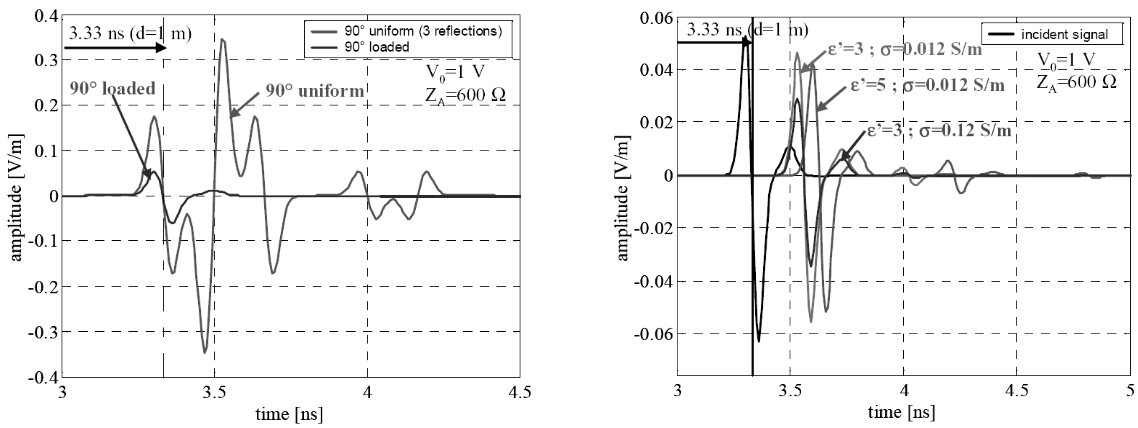

(a) Electric field radiated in the far-field zone from uniform and loaded V-dipoles ($2L = 20\,\mathrm{cm}$).

(b) Electric field radiated from a loaded V-dipole and transmitted through a single-layer sample ($e = 4\,\mathrm{cm}$).

Figure 3: (a) Waveforms radiated by uniform and loaded V-dipoles; (b) Resulting waveforms radiated by a loaded V-dipole and transmitted through a single-layer dielectric sample ($e = 4\,\mathrm{cm}$).

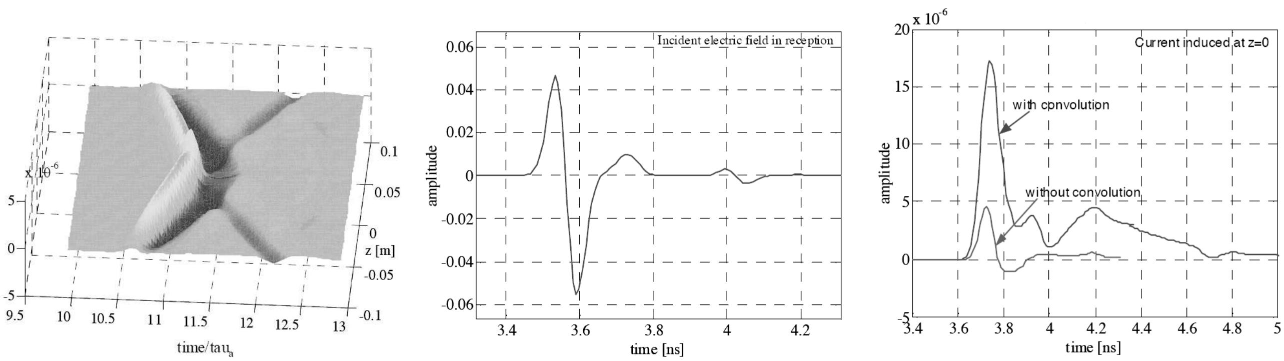

(a) (b) (c)

Figure 4: (a) 3D current distribution along the V-dipole ($2\alpha = 120°$, L=10 cm, incidence $\varphi = 0°$ so $\Psi = 30°$); (b) Current distribution induced in a loaded V-dipole in the reception configuration considering the incident wavefront (a); (c) Detected current at the position z=0.

3 reflections) and a loaded V-dipole of the same dimensions have been compared; the plots of Figure 3a which consider the direction $\theta = 90°$ show that as the uniform V-dipole gives a distorted version of the excitation signal with a ringing phenomenon, the loaded V-dipole generates an attenuated and a slightly distorted version of the initial pulse. Then, we have studied the transmission of the signal radiated by the loaded dipole under the incidence angle $\theta_i = 0°$ and through a single layer material considering the following dielectric properties: (1) $\epsilon' = 3$, $\sigma = 0.012\,\mathrm{S\cdot\ m^{-1}}$, (2) $\epsilon' = 3$, $\sigma = 0.12\,\mathrm{S\cdot\ m^{-1}}$, and (3) $\epsilon' = 5$, $\sigma = 0.012\,\mathrm{S\cdot\ m^{-1}}$. The resulted waveforms can be visualized in Figure 3(b). The corresponding ratios of the energy transmitted to the energy of the incident signal are respectively 77.7%, 30.3%, and 68.5%. So, these results highlight the strong attenuation e!ect introduced by the losses produced inside the material. Afterwards, considering the signal transmitted through the sample with the dielectric properties $\epsilon' = 3$, $\sigma = 0.012\,\mathrm{S\cdot\ m^{-1}}$ (see Figure 4(b)), we have computed the current distribution in a loaded V-dipole ($\beta = 30°$). The 3D plot of Figure 4(a) shows the induced current before executing the convolution product with the term e^{-t/τ_n} and mentioned in relation (16). The current at the position $z = 0$ is visualized in Figure 4(c) before and after the convolution operation. We remark that such an operation smoothes the signal.

4. Conclusion

In this paper, the modelling of a communication link involving two transmitting and receiving antennas in the time domain has been revisited. The modelling, based on analytical expressions, allows to consider several conductive antennas which can be represented by a simplified model using a combination of non interacting thin-wire elements. Further developments have been made mainly in the reception configuration in order to consider the interaction of a uniform or a loaded Wu and King dipole which are supposed to be illuminated by an oblique plane wavefront. At present, the propagation channel has been represented by the presence of a multi-layer dielectric dispersive material which produces multipath induced by the multiple reflections occuring in its thickness. Statistical models of propagation channel, such as the Turin approach, associated in a given environment can be planned. Samples of the parametric studies made have been presented in the case of a communication link involving two transmitting and receiving V-dipoles. We have particularly analyzed the case of a WK V-dipole as its better represents an UWB band as the ringing effect of the current has been eliminated by a distributed absorption along each arm. The realization of a graphical interface will make easier more parametric studies to thoroughly analyzed the link budget in a given configuration. Moreover, optimization of the link will be addressed.

REFERENCES

1. Bantin, C. C., "Pulsed communications link between dipoles," *IEEE Antennas and Propagat. Magazine*, Vol. 44, No. 5, 75–82, October 2002.
2. Sagnard, F., "Propagation and radiation studies for the development of the future communication systems," Habilitation à Diriger des Recherches, University of Marne-La-Vallée, France, 23 March, 2005.
3. Martin, R. G. and J. A. Morente, "An approximate analysis of transient radiation from linear antennas," *Int. Journal Electronics*, Vol. 61, No. 3, 343–353, 1988.
4. Wu, T. T. and R. W. P. King, "The cylindrical antenna with non-reecting resistive loading," *IEEE Trans. Antennas Propagat.*, Vol. 13, 369–373, May 1965.
5. Samaddar, S. N. and E. L. Mokole, "Transient behaviour of radiated and received fields associated with a resistively loaded dipole," *Ultra-Wideband Short Pulse Electromagnetics 4*, Herman et al., Kluwer, 165–179, 1999.
6. Sagnard, F. and C. Vignat, "Extension of the analytical modelling of resistive loaded thin-wire antennas to Gaussian derivatives excitations," *Microwave Optical Technology Letters*, Vol. 47, No. 6, 548–553, December 2005.